Rapid Effects of a Protective O-Polysaccharide-Specific Monoclonal IgA on *Vibrio cholerae* Agglutination, Motility, and Surface Morphology

Kara J. Levinson,[a,b] Magdia De Jesus,[a] Nicholas J. Mantis[a,b]

Division of Infectious Diseases, Wadsworth Center, New York State Department of Health, Albany, New York, USA[a]; Department of Biomedical Sciences, University at Albany, Albany, New York, USA[b]

2D6 is a dimeric monoclonal immunoglobulin A (IgA) specific for the nonreducing terminal residue of Ogawa O-polysaccharide (OPS) of *Vibrio cholerae*. It was previously demonstrated that 2D6 IgA is sufficient to passively protect suckling mice from oral challenge with virulent *V. cholerae* O395. In this study, we sought to define the mechanism by which 2D6 IgA antibody protects the intestinal epithelium from *V. cholerae* infection. In a mouse ligated-ileal-loop assay, 2D6 IgA promoted *V. cholerae* agglutination in the intestinal lumen and limited the ability of the bacteria to associate with the epithelium, particularly within the crypt regions. *In vitro* fluorescence digital video microscopy analysis of antibody-treated *V. cholerae* in liquid medium revealed that 2D6 IgA not only induced the rapid (5- to 10-min) onset of agglutination but was an equally potent inhibitor of bacterial motility. Scanning electron microscopy showed that 2D6 IgA promoted flagellum-flagellum cross-linking, as well as flagellar entanglement with bacterial bodies, suggesting that motility arrest may be a consequence of flagellar tethering. However, monovalent 2D6 Fab fragments also inhibited *V. cholerae* motility, demonstrating that antibody-mediated agglutination and motility arrest are separate phenomena. While 2D6 IgA is neither bactericidal nor bacteriostatic, exposure of *V. cholerae* to 2D6 IgA (or Fab fragments) resulted in a 5-fold increase in surface-associated blebs, as well an onset of a wrinkled surface morphotype. We propose that the protective immunity conferred by 2D6 IgA is the result of multifactorial effects on *V. cholerae*, including agglutination, motility arrest, and possibly outer membrane stress.

Cholera is a life-threatening disease that remains endemic in many parts of the world (1–3). The etiological agent of cholera, *Vibrio cholerae*, is a noninvasive, Gram-negative bacterium that is acquired by humans via the fecal-oral route. Following ingestion, *V. cholerae* colonizes the mucosal surfaces of the small intestines, a process that is facilitated by the bacterium's single polar flagellum (4–7). Adherence to the epithelial surface requires expression of the toxin-coregulated pilus (TCP), in addition to other virulence factors (8), most notably, a potent ADP-ribosylating toxin known as cholera toxin (CT). CT disrupts chloride secretion within intestinal epithelial cells, inducing profuse water and electrolyte secretion and ultimately resulting in the hallmark "rice water diarrhea" associated with cholera. Cholera outbreaks frequently occur when water sanitation is disrupted, either following natural disasters or seasonally in areas where *V. cholerae* is endemic (9). The recent cholera outbreak in Haiti following the 2010 earthquake highlighted the ongoing potential of *V. cholerae* to cause mass causalities, as it resulted in more than half a million infected individuals and more than 7,000 deaths (10). Due to the rapid onset of symptoms and limited treatment options, control of cholera in many parts of the globe, particularly where it is endemic, will be achieved only through vaccination (10).

Immunity to *V. cholerae* is primarily antibody mediated. While natural *V. cholerae* infection, as well as oral vaccination, induces both IgA and IgG antibody responses, secretory IgA (S-IgA) antibodies directed against bacterial surface antigens, especially lipopolysaccharide (LPS) are considered the primary determinants of protection (1, 9). Work by the laboratories of John Mekalanos and Marian Neutra more than 20 years ago established that IgA antibodies alone, when actively transported or passively applied into the intestinal lumen, are sufficient to protect suckling mice from

lethal *V. cholerae* challenge (11, 12). Protection was associated with antibodies directed against LPS and not CT, even though antitoxin antibodies were able to neutralize CT *in vitro* (11). Others have confirmed the importance of LPS-specific IgA in interfering with *V. cholerae* colonization of the intestinal epithelium in the neonatal mouse model and with tissue section overlay assays (13–16). LPS-specific fecal IgA levels are also implicated as a primary correlate of immunity to *V. cholerae* in humans (3, 17–19).

Despite the evidence that LPS-specific IgA antibodies play a central role in protective immunity to *V. cholerae*, it is still not clear how they impede the ability of the bacterium to colonize the intestinal epithelium. IgA is not vibriocidal, nor does it promote Fc-mediated uptake of opsonized bacteria in the intestinal lumen (12). LPS-specific IgA antibodies, however, are effective at promoting bacterial agglutination *in vitro*, which led Winner and colleagues to propose that IgA might aggregate and entrap vibrios in

the intestinal lumen and thereby limit their access to the epithelial surface through a phenomenon known as immune exclusion (12, 20).

There is emerging evidence to suggest that protective anti-LPS IgA antibodies may have direct effects on microbial virulence, independent of agglutination (20–24). In the case of *V. cholerae*, Bishop and Camilli demonstrated using dark-field microscopy that polyclonal anti-LPS IgA antibodies inhibit *V. cholerae* motility *in vitro*, an observation that has been confirmed by others (13, 14). Visually, IgA-mediated motility arrest of *V. cholerae* occurred before the bacteria became agglutinated, suggesting that the two phenomena are distinct. In the case of *Salmonella enterica* serovar Typhimurium, we reported in 2008 that treatment of *S.* Typhimurium with a protective O-antigen-specific IgA monoclonal antibody (MAb) known as Sal4 results in the immediate arrest of flagellum-based motility, independent of agglutination (23). More recently we demonstrated that Sal4 triggers a reduction in type 3 secretion system (T3SS) activity and alterations in outer membrane integrity and onset of exopolysaccharide (EPS) production. From these data, we have postulated that Sal4 triggers an outer membrane stress response in *S.* Typhimurium that temporarily renders the bacterium avirulent (24). We are only beginning to investigate whether LPS-specific IgA antibodies have similar effects on other enteric pathogens.

In this report, we have probed the interaction between *V. cholerae* and 2D6, a murine IgA MAb directed against the immunodominant nonreducing terminal residue of Ogawa O-polysaccharide (OPS) (9, 11, 12, 25). 2D6 was the first IgA MAb shown to be sufficient to protect suckling mice from a lethal challenge of *V. cholerae* (12). Here we provide evidence that 2D6 limits *V. cholerae* colonization of the intestinal epithelium through a combination of agglutination, antibody-mediated motility arrest, and, possibly, even outer membrane stress.

(Parts of this work were presented at the 114th General Meeting of the American Society for Microbiology, Boston, MA, May 2014 [26].)

MATERIALS AND METHODS

Bacterial strains and growth conditions. All strains used in this study are derivatives of the *V. cholerae* O1 classical strain O395, which was a gift from John Mekalanos (Harvard Medical School) (27). Strain RT4273 consists of *V. cholerae* O395 containing the plasmid pGreenTIR (28) and was kindly provided by Ronald Taylor (Dartmouth Medical School). Strains were grown in LB medium at 37°C with aeration (150 rpm) supplemented when necessary with ampicillin (100 μg/ml).

Antibodies. Rabbit polyclonal antisera against the *V. cholerae* Inaba and Ogawa antigens were purchased from BD Difco (Franklin Lakes, NJ) and dialyzed against phosphate-buffered saline (PBS) with a Slide-A-Lyzer (10,000-molecular-weight cutoff; Pierce Scientific, Rockford, IL) prior to use. The monoclonal dimeric IgA antibodies Sal4 (specific for the *Salmonella enterica* serovar Typhimurium O5 antigen) (29) and 2D6 (specific for *V. cholerae* OPS) (12) were obtained from Marian Neutra (Children's Hospital, Boston, MA). Sal4 and 2D6 hybridomas were maintained in CD hybridoma serum-free, protein-free medium (Gibco-Invitrogen, Carlsbad, CA) without antibiotics at 37°C in a 5% CO_2–95% air atmosphere, as described previously (23). The concentrations of Sal4 and 2D6 were determined by sandwich enzyme-linked immunosorbent assay with IgA TEPC-15 (Sigma-Aldrich, St. Louis, MO) as a standard. As mouse IgA is refractory to protease digestion with papain, Fab fragments were generated from a recombinant chimeric derivative of 2D6 in which the mouse heavy- and light-chain (H+L) variable regions were grafted onto an IgG1 backbone (K. Levinson, M. Pauly, K. Whaley, L. Zeitlin, and N. Mantis,

unpublished data). Fab fragments of chimeric 2D6 IgG were produced using the IgG Fab preparation kit (ThermoScientific, Rockford, IL). SDS-PAGE and GelCode Blue (ThermoScientfic) staining were used to confirm that MAb 2D6 IgG was digested to completion. Fab fragments were measured by NanoDrop (ThermoScientific, Wilmington, DE) to determine the concentration.

Mouse ligated-ileal-loop assays. Female BALB/c mice (5 to 8 weeks old) were obtained from Taconic (Hudson, NY). Animals were housed under conventional specific-pathogen-free conditions and were treated in compliance with the Wadsworth Center's Institutional Animal Care and Use Committee (IACUC) guidelines. The ligated-ileal-loop assays were conducted essentially as described previously (30). Briefly, mice under isoflurane anesthesia were subjected to a laparotomy to expose a 1- to 2-cm segment of the ileum containing a single Peyer's patch. *V. cholerae* O395 (1.5×10^8 cells/0.2 ml) mixed with the indicated MAbs or Fab fragments (9 μg/ml) and was injected into the ligated ileal loops. After 30 min, the animal was euthanized, and intestinal segments were removed, embedded in OCT medium, and snap-frozen in liquid nitrogen (31). Serial cryosections (25 μm) of frozen tissue were prepared using a Reichert-Jung 2800e cryostat (Leica, Wetzlar, Germany) and stained. For each experiment, we used at least two mice per treatment group (e.g., control, Sal4, and 2D6), and the experiments were repeated three independent times.

To detect *V. cholerae*, we stained the tissue with polyclonal rabbit anti-LPS antisera (BD, Sparks, MD) and used goat anti-rabbit Alexa Fluor 546 IgG (H+L) (Molecular Probes, Eugene, OR) as a secondary antibody. To stain for dendritic cells, we used anti-mouse CD11c-allophycocyanin (APC) conjugate clone N418 (eBioscience, San Diego, CA). Sections were visualized using a Leica SP5 confocal laser scanning microscope (Leica, Wetzlar, Germany) and processed using Fiji (ImageJ) software version 1.49f (32). Montage confocal images were generated using Adobe Photoshop version 13.0 ×32 (San Jose, CA).

***V. cholerae* motility and agglutination assays.** *V. cholerae* liquid motility assays were conducted as follows. Mid-log-phase cultures of strain RT4273 were treated with the indicated MAbs (15 μg/ml) and then spotted (30 μl) onto glass microscope slides with a coverslip. The slides were immediately mounted on a Nikon TI inverted microscope equipped with a CoolSnap HQ2 camera (Photometrics, Tucson, AZ). In an effort to minimize the photon dose to the bacteria, the illumination was shuttered, and we used a monochrome camera. Cells were imaged using a 60× objective (1.4 NA) with immersion oil and monitored for a total of 30 min. Every 5 min, we acquired three videos, each containing 100 image sequences (110 ms of exposure/frame). Within each 100-frame video, frames 20 to 25, 60 to 65, and 80 to 85 were visualized using Fiji software version 1.49f (32). Motility was determined by manually tracking individual bacteria across each of the six-frame snapshots. We used the mean fluorescence intensity (MFI) determinations of bacterial clusters to estimate the degree of bacterial agglutination in each of the six-frame snapshots. The video microscopy experiments were conducted three independent times, and then the results were averaged.

SEM. For scanning electron microscopy (SEM), mid-log-phase cultures of *V. cholerae* O395 were diluted 1:50 into 2 ml of LB broth containing 9 μg/ml of Sal4 IgA, 2D6 IgA, 2D6 IgG, or 2D6 Fab fragments and incubated at 37°C for 20, 60, or 120 min with aeration (150 rpm). Samples were captured on 0.2-μm-pore polycarbonate filters using a vacuum apparatus and fixed with 2% glutaraldehyde for 20 min, washed with PBS and sterile water, and then subjected to a series of ethanol dehydrations (5 min each). The samples were critical point dried, mounted on aluminum studs with carbon paste, and sputter coated with gold for 45 s. Samples were imaged on a Zeiss Neon-40 EsB FIB-SEM.

RESULTS

2D6 IgA promotes *V. cholerae* agglutination and interferes with epithelial attachment in a mouse ligated-ileal-loop model. To examine whether 2D6 IgA interfered with the ability of *V. cholerae*
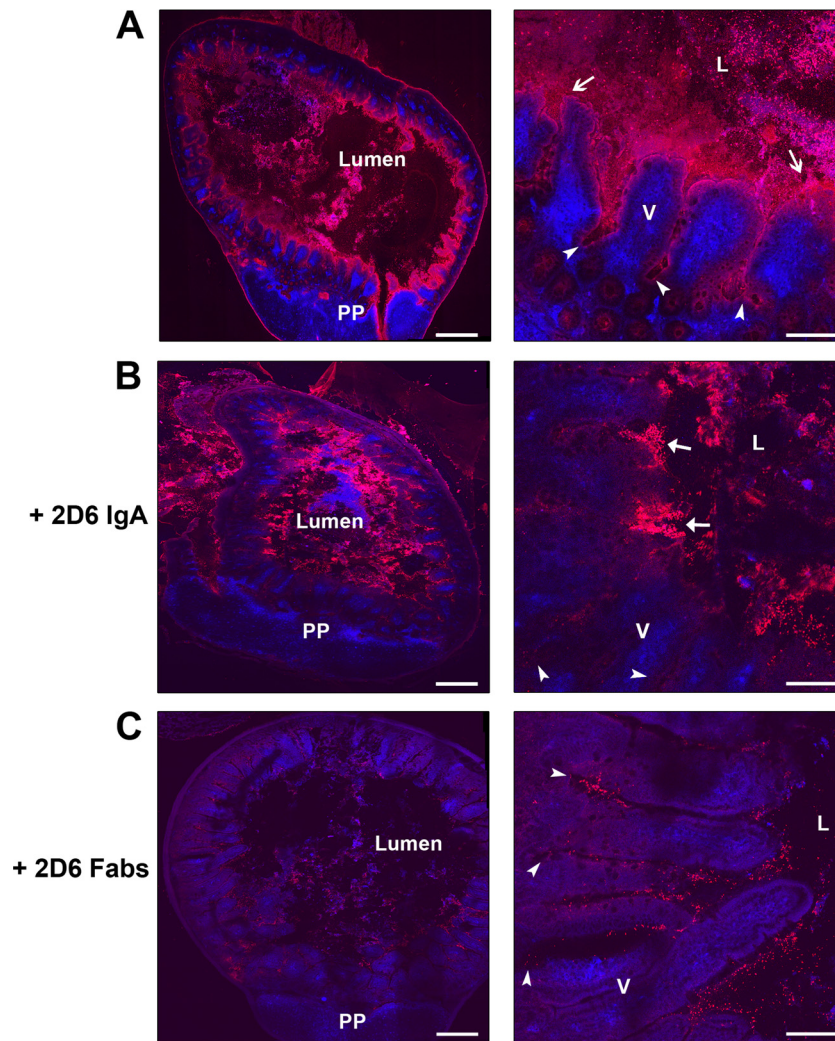
FIG 1 2D6 IgA reduces *V. cholerae* attachment to epithelial surfaces *in vivo*. *V. cholerae* O395 was either untreated (A) or treated with 2D6 IgA (B) or 2D6 Fab fragments (C) and injected into 1-cm ligated ileal loops of BALB/c mice, as described in Materials and Methods. After 30 min, the loops were excised, frozen, cryosectioned, and stained with fluorescently labeled *V. cholerae* antiserum (red) or CD11c (blue) to detect mucosal dendritic cells (DCs). Stained cryosections were then visualized by confocal microscopy. In each case, the panels in the right-hand column are zoomed-in images of the panels in the left-hand columns. In panels A, *V. cholerae* was observed in close association with the epithelium (arrows) and penetrating the intestinal crypts (arrowheads). In panels B, 2D6 IgA-treated bacteria were largely aggregated in the lumen (arrows) and rarely in the crypts (arrowheads). In panels C, 2D6 Fab fragment-treated *V. cholerae* cells were observed in close association with villus epithelium and in the crypts (arrowhead). Scale bars, left column, 300 μm; right column, 50 μm. Abbreviations: PP, Peyer's patches; V, villi; L, lumen.

cells to adhere to and colonize the intestinal epithelium, strain O395 was mixed with 2D6 or the *S.* Typhimurium-specific IgA antibody Sal4 as an isotype control and then injected into mouse ligated ileal loops. In control samples, we observed *V. cholerae* situated within the intestinal lumen as well as in close proximity to the villus epithelium. In the lumen, bacteria were uniformly distributed throughout and were rarely aggregated or clumped (Fig. 1A). In proximity to the epithelium, bacteria were concentrated at the tips of villi (likely within the mucus) as well as lower aspects of villi and crypts. *V. cholerae* was occasionally observed associated with the follicle-associated epithelium (FAE) of Peyer's patches. In contrast, 2D6-treated bacteria were retained in the intestinal lumen, either as large aggregates or as clusters of cells (Fig. 1B). Although the ligated-ileal-loop assay was not quantitative, we noted (based on relative fluorescence intensity) that bacteria

treated with 2D6 were less frequently associated with the intestinal epithelium or crypts than the control Sal4-treated bacteria. These data demonstrate that 2D6 interferes with the ability of *V. cholerae* to adhere to the intestinal epithelium.

2D6 IgA promotes *V. cholerae* agglutination and motility arrest *in vitro*. Having demonstrated that 2D6 promotes bacterial agglutination within the intestinal lumen, we postulated that the antibody might have additional effects on the capacity of *V. cholerae* to colonize epithelial surfaces. Bishop and Camilli reported that polyclonal LPS-specific IgA antibodies were potent inhibitors of *V. cholerae* motility (13). To determine if 2D6 IgA has an effect on *V. cholerae* motility, mid-log-phase cultures of green fluorescent protein (GFP)-expressing strain RT4273 were treated with 2D6, spotted onto glass microscope slides, and imaged by digital video fluorescence microscopy. In untreated control cul-
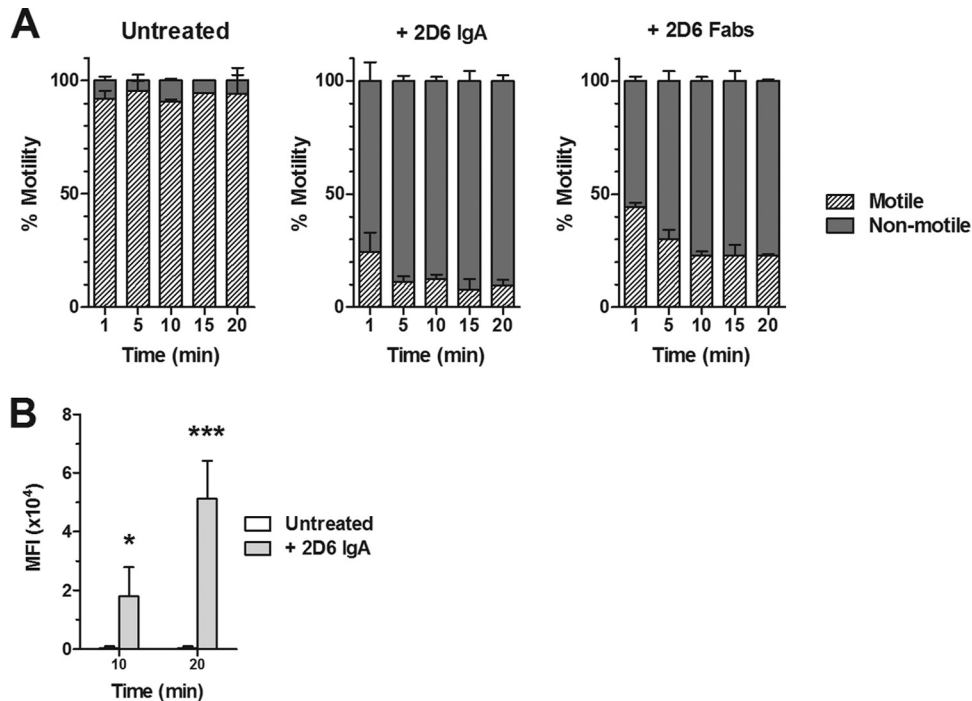
FIG 2 2D6 IgA rapidly inhibits *V. cholerae* motility in liquid media. A mid-log-phase culture of *V. cholerae* strain RT4273 was treated with 2D6 IgA or 2D6 Fab fragments, spotted onto a microscope slide, mounted on Nikon TI inverted microscope equipped with a CoolSnap HQ2 digital camera, and imaged for 20 min, as described in Materials and Methods. (A) Quantitation (percentage) of the number of motile and nonmotile cells at each time point following antibody treatment. There was a significant reduction ($P < 0.01$, Student's *t* test) in bacterial motility following treatment of *V. cholerae* with 2D6 IgA or 2D6 Fab fragments at all time points examined compared to control (untreated) cells. (B) Assessment of bacterial agglutination by measurement of mean fluorescent intensity (MFI) following 2D6 IgA treatment. In the absence of 2D6 IgA, there was no measurable agglutination. Student's *t* test was used to determine significance (*, $P < 0.05$; ***, $P = 0.0003$).

tures, *V. cholerae* remained motile (>95%) and free of any detectable agglutination for the entire 30-min observation period (Fig. 2; see Movie S1 in the supplemental material). The addition of Sal4 as an IgA isotype control did not influence *V. cholerae* motility or agglutination (data not shown). In contrast, 2D6 IgA treatment resulted in a rapid and dose-dependent inhibition of *V. cholerae* motility that occurred in advance of or concordant with the onset of agglutination (Table 1 and Fig. 2; see Movie S2 in the supplemental material). By 5 min, >85% of the cells in culture were immobilized: approximately half of the nonmotile bacteria were associated with clusters consisting of ~3 to 10 bacterial bodies, while the remainder were single cells. Most notably, we observed numerous single cells that rapidly transitioned from motile to nonmotile upon antibody treatment, a finding that supports the claim of Bishop and Camilli that motility arrest can occur independently of agglutination (13). Furthermore, we observed bacteria wriggling within the clusters, suggesting that flagellar rotation is not fully extinguished even when the cells are bound to each other (Table 1 and Fig. 2; see Movie S2). By 30 min, virtually all cells within the 2D6 IgA-treated cultures were amassed into large macroscopic aggregates and were completely devoid of movement. Collectively, these data demonstrate that 2D6 IgA-mediated agglutination and motility arrest of *V. cholerae* occur rapidly and are likely distinct phenomena.

TABLE 1 Differential impact of different 2D6 antibody types on *V. cholerae*[a]

| 2D6 antibody type | Valency | Agglutination | Motility | | SEM result[d] |
			Semisolid agar[b]	Liquid medium[c]	
IgA	4	++++	+++	++++	W, B, T
IgG1	2	+	+	++	W, B, T
Fab fragments	1	−	+	++	W, B

[a] Mid-log-phase cultures of *V. cholerae* strain RT4273 were mixed with 2D6 antibody (9 μg/ml) and visualized by confocal microscopy after 30 min of incubation. The degree of agglutination or motility arrest was scored as follows: ++++, >85%; +++, >70%; ++, >50%; +, >20%; −, 0%.
[b] *V. cholerae* O395 was stabbed into 0.3% semisolid agar containing 2D6 antibody (9 μg/ml) and then incubated at 37°C. Migration away from the stab site was measured after 8 h of incubation at 37°C. The values indicate the degree to which the different antibody preparations inhibited bacterial migration compared to that of isotype controls.
[c] Shown is bacterial motility inhibition in liquid medium. The data presented in this column represent a summary of data from Fig. 2 and from Movies S2 to S4 in the supplemental material.
[d] SEM, scanning electron microscopy; W, wrinkling; B, blebbing; T, tethering. The data presented in this column represent a summary from Fig. 3, 4, and 5.

2D6 IgA promotes bacterial cross-linking and induces changes in *V. cholerae* surface morphology. *V. cholerae*'s single polar flagellum generates extraordinary torque, as it can propel the bacterium at speeds of >70 µm/s (33). To examine how a single MAb directed against OPS interferes with *V. cholerae* flagellum-mediated motility in such a rapid and potent manner, we treated *V. cholerae* with 2D6 IgA and imaged the cells by SEM. Mid-log-phase cultures of *V. cholerae* O395 were incubated with 2D6 IgA for 20, 60, or 120 min, after which they were collected by vacuum filtration, fixed, critical point dried, coated with gold, and visualized by SEM. Control (Sal4-treated) *V. cholerae* O395 cells were evenly distributed across the porous filter with no evidence of bacterial agglutination or clumping (Fig. 3A and B). In general, the surfaces of the bacteria were smooth and relatively devoid of blebs. Furthermore, formation of septa was apparent on numerous bacterial bodies, indicating that the cells were undergoing division at the time of chemical fixation. We only observed flagella on a small fraction of *V. cholerae* cells, possibly as a result of mild shear forces encountered during processing for SEM (34).

The appearance of cells treated with 2D6 IgA was strikingly different. As early as 20 min following 2D6 IgA exposure, *V. cholerae* cells were completely aggregated—likely a result of antibody-mediated cross-linking (Fig. 3C and D). Flagella were wrapped around and sandwiched between neighboring bacterial cells as well as entangled, looped, and knotted with other flagella (Fig. 3D). The formation of cell-flagellum and flagellum-flagellum interactions may explain, in part, the rapid capacity of 2D6 IgA to promote the *V. cholerae* motility arrest and agglutination we observed by video light microscopy.

The surfaces of the 2D6-treated *V. cholerae* cells were also notably more wrinkled than those of the Sal4-treated cells, and there was a significant increase in the number of membrane-associated blebs (Fig. 3D and 4). Blebs observed on the surface of control (Sal4-treated) cells tended to be small and more homogenous in size (40 to 60 nm in diameter), whereas following 2D6 IgA treatment, the surface blebs were larger and more heterogeneous in size, ranging from 30 to 160 nm in diameter. By 120 min, 2D6 IgA-treated *V. cholerae* cells remained tethered to each other via flagella and assumed a crusty appearance (Fig. 3E). There was also a notable increase in debris associated with the cell poles and filter surfaces, possibly indicative of sloughing of blebs or other surface materials. Collectively, these images suggest that 2D6 may induce a form of outer membrane stress in *V. cholerae*, despite the fact that 2D6 IgA is neither bactericidal nor bacteriostatic (data not shown).

Motility arrest and changes in surface morphology induced by monovalent 2D6 Fab fragments. To further examine the mechanism by which 2D6 promotes motility arrest and alterations in *V. cholerae* surface morphology independent of antibody-mediated cross-linking, we generated monovalent 2D6 Fab fragments. Mid-log-phase cultures of *V. cholerae* GFP-expressing strain RT4273 were mixed with 2D6 IgA, 2D6 IgG, or 2D6 Fab fragments, spotted onto glass microscope slides, and then imaged by video fluorescence microscopy, as described above. As observed previously, 2D6 IgA treatment arrested *V. cholerae* motility within 5 min and was accompanied by agglutination. By 30 min, cultures treated with IgA 2D6 were completely immobilized (see Movie S2 in the supplemental material). 2D6 IgG had a similar, albeit slower effect on *V. cholerae* motility arrest (Table 1; see Movie S3 in the supplemental material), indicating that the di-

meric nature of 2D6 IgA (as opposed to the monomeric nature of 2D6 IgG) likely contributes to 2D6's biological activity. Finally, although 2D6 Fab fragments did not induce agglutination or tethering of *V. cholerae*, they were able to promote motility arrest. Within 5 min, approximately 50% of Fab-treated cells were immobilized, and by 20 min, >70% were nonmotile (Table 1; see Movie S4 in the supplemental material).

To investigate whether 2D6 Fab fragments were sufficient to induce changes in *V. cholerae* surface morphology, mid-log-phase cultures of *V. cholerae* were treated with 2D6 Fab fragments and then subjected to SEM, as described above. As expected, treatment of cells with 2D6 IgA induced agglutination, flagellar interactions, surface blebbing, and wrinkling. We observed that treatment of *V. cholerae* with 2D6 Fab fragments elicited membrane blebs and wrinkles that were virtually identical to those observed on 2D6 IgA-treated cells (Fig. 5). Between 60 and 120 min, Fab-treated cells assumed a crusty appearance similar to what we had observed following IgA 2D6 treatment (Fig. 3E). These data demonstrate that binding of 2D6 to the surface of *V. cholerae*, in the absence of cross-linking or agglutination, is sufficient to arrest bacterial motility and to promote changes in surface morphology.

We next employed the mouse ligated-ileal-loop assay to investigate the effects of 2D6 Fabs on the ability of *V. cholerae* to colonize epithelial surfaces. As expected, 2D6 Fab-treated cells were not overtly aggregated in the lumenal space (Fig. 1C), which was in stark contrast to what was observed when bacteria where treated with 2D6 IgA. Moreover, we observed that bacteria treated with 2D6 Fabs were distributed along the length of individual intestinal villi and were present in crypts, demonstrating that the Fab fragments alone (and presumably their effects on motility and surface morphology) were not sufficient to prevent bacterial access to target niches. However, one caveat to these studies is that the mouse ligated-ileal-loop assay is not necessarily an ideal model system with which to assess the contribution of flagellum-based motility, as evidenced by the fact that a *V. cholerae* ΔflaA mutant was similar to wild-type O395 in its ability to visibly associate with villus and crypt epithelium (see Fig. S1 in the supplemental material).

DISCUSSION

Although there is mounting evidence that OPS-specific IgA antibodies are the primary contributor to mucosal immunity against *V. cholerae*, the mechanisms by which these antibodies interfere with *V. cholerae*'s ability to colonize the intestinal epithelium remain poorly understood (3, 9, 17–19, 35). In this study, we examined the interaction between *V. cholerae* O395 and 2D6, a murine polymeric IgA MAb directed against the nonreducing terminal residue of Ogawa OPS (11, 12, 25). 2D6 was the first monoclonal IgA shown to be sufficient to protect suckling mice from a lethal challenge with *V. cholerae* and, therefore, serves as an invaluable tool to elucidate the impact of secretory IgA antibodies on *V. cholerae* virulence and pathogenesis (12).

Using a mouse ligated-ileal-loop assay, we observed that 2D6 IgA limited the ability of *V. cholerae* to visibly associate with the intestinal epithelium, particularly within the crypt regions. Whereas control bacteria were uniformly distributed across the apical aspects of the small intestine, including the crypts, 2D6-treated cells were observed as large aggregates and microclusters largely confined to the lumen. Under the same experimental conditions, monovalent 2D6 Fab fragments did not noticeably inter-
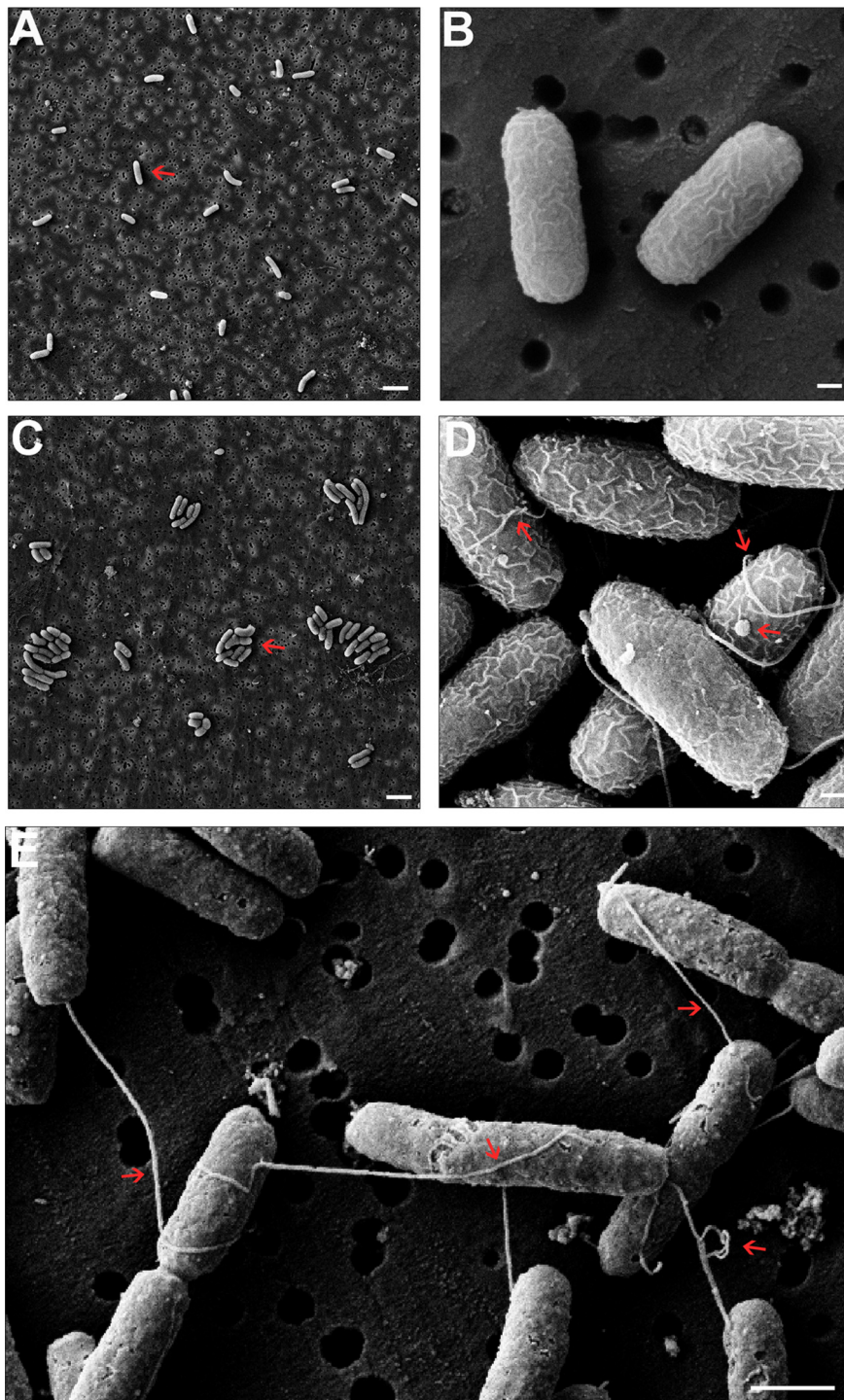
FIG 3 SEM analysis reveals that 2D6 IgA treatment induces membrane wrinkling, blebbing, and flagellar tethering. Mid-log-phase cultures of *V. cholerae* O395 were treated with Sal4 IgA (A and B) or 2D6 IgA (C to E). Cells were collected at 20 min (A and C), 60 min (B and D), or 120 min (E) following antibody treatment and processed for SEM, as described in Materials and Methods. (A and B) Control-treated *V. cholerae* cells were evenly distributed across the porous filter membrane, and there was no evidence of bacterial agglutination or clumping. (C to E) Compared to control cells, 2D6 IgA-treated *V. cholerae* cells were aggregated (compare arrows in panels A and C) and were notably more wrinkled (compare panels B and D). In addition, following 60 min (D) and 120 min (E) of treatment with 2D6 IgA, there was notable flagellum-flagellum cross-linking, flagellar entanglement with neighboring bacterial bodies, and even flagellar knotting (arrows). (D) *V. cholerae* cells treated with 2D6 IgA were also associated with an increased number of surface blebs (arrow). Note that TCP was not observed in these images, because the bacteria were cultured under non-toxin-inducing conditions. Scale bars: panels A and C, 2 μm; panels B and D, 200 nm; panel E, 1 μm.
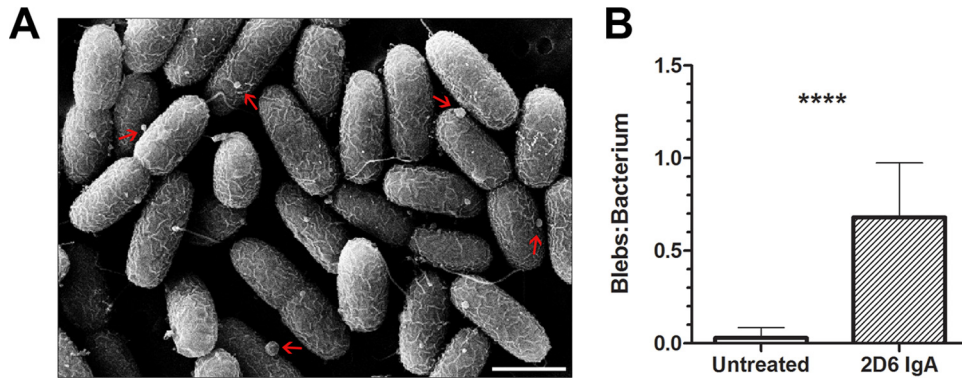
FIG 4 Increased blebs on the surface of *V. cholerae* following 2D6 IgA treatment. Mid-log-phase cultures of *V. cholerae* O395 were treated with 2D6 IgA for 60 min and then processed for SEM, as described in the legend to Fig. 3. (A) Surface blebs (arrows) on cells following 2D6 IgA treatment. Scale bar, 1 μm. (B) Quantitation of blebs per bacterium in control or 2D6 IgA-treated *V. cholerae*. In general, blebs were heterogeneous in size (30 to 160 μm) following 2D6 IgA treatment compared to those in control cells, where they were less numerous and more homogenous (40 to 60 μm). Student's *t* test was used to determine significance ($P < 0.0001$).

fere with *V. cholerae*-epithelial contact, underscoring the importance of agglutination in limiting bacterial association with the intestinal epithelium, at least in the mouse ligated-ileal-loop model. In line with what is known about S-IgA in the human host, it would be expected that 2D6 IgA-mediated cross-linking of *V. cholerae* would result in bacterial entrapment in mucus and clearance from the intestine via peristalsis (11, 12, 36). The secretory component (SC), which has known mucophilic properties, would further enhance 2D6 IgA's capacity to ensnare *V. cholerae* within the mucus layer (37).

The extent to which agglutination contributes to protective immunity to *V. cholerae* during infection (as opposed to the ligated-ileal-loop assay) remains unresolved (38). Agglutination is likely a rare event *in vivo*, considering that formation of bacterium-antibody cross-linked complexes is achieved only when the stoichiometry of bacteria to specific antibody is optimal. Even a relatively high inoculum of *V. cholerae* ($>10^6$) would be expected to become diluted considerably within the contents of the stomach and further dispersed along the length of the proximal small intestine, making the likelihood of forming bacterium-antibody bridges slim. Moreover, there may even be less opportunity for bacterial cross-linking to occur than previously assumed in light

of recent work indicating that colonization of epithelial surfaces by *V. cholerae* is initiated by single seeder cells and not microclusters (6).

With that in mind, the observation that 2D6 IgA inhibits *V. cholerae* O395 motility *in vitro* should be considered a possible determinant of protective immunity *in vivo*. By fluorescence digital video microscopy, we noted that exposure of *V. cholerae* to 2D6 IgA resulted in a majority (>85%) of cells becoming immobilized within 5 min; by 30 min the entire cell population had come to a standstill. Although Gustafsson and Holme recognized the inhibition of *V. cholerae* motility by anti-LPS antibodies 30 years ago (39), it is only recently that motility arrest has been associated with mucosal protection. Specifically, Bishop and Camilli demonstrated by dark-field microscopy that milk-derived mouse polyclonal anti-LPS IgA antibodies inhibited bacterial motility in aqueous medium and that this activity correlated with protection in the neonatal mouse model (13). They also noted that that motility arrest appeared to precede agglutination, suggesting that the two phenomena (i.e., motility arrest and agglutination) are in fact distinct events.

Our study advances the work by Bishop and Camilli in two important ways. First, we established that targeting IgA to a single
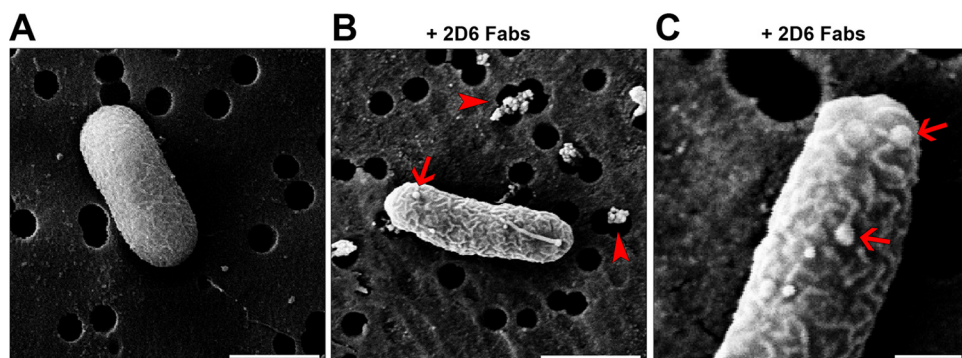
FIG 5 Treatment of *V. cholerae* with 2D6 Fab fragments results in membrane wrinkles and blebs. Mid-log-phase cultures of *V. cholerae* O395 were treated with 2D6 Fab fragments for 60 min and then processed for SEM, as described in the legend to Fig. 3. (A) Control cell with relatively smooth surface pattern and single polar flagellum. (B and C) Cells treated with 2D6 Fab fragments were wrinkled and had numerous blebs (arrows), similar to those observed following 2D6 IgA treatment. Moreover, there was notable debris on the filter surface (arrowheads) that was absent from the control cells. Scale bars: panels A and B, 1 μm; panel C, 200 nm.

epitope on the serotype-specific terminal residue of Ogawa OPS is sufficient to promote *V. cholerae* motility arrest. Previously only polyclonal IgA antibodies of mixed epitope specificity and unknown concentrations had been evaluated in motility studies (13). 2D6 is one of only two murine monoclonal IgAs against *V. cholerae* LPS that have been described in the literature. The other, MAb ZAC-3, recognizes an epitope within the lipid A and/or core regions of LPS common to Ogawa and Inaba (25). Interestingly, our preliminary studies suggest that ZAC-3 is significantly more effective than 2D6 at inhibiting bacterial motility *in vitro* (K. Levinson, S. Giffen, and N. Mantis, unpublished results), raising the possibility that epitope specificity may influence antibody potency. Defining the relationships between epitope specificity, motility arrest, and, ultimately, protective immunity could have important implications for cholera vaccine development and assessment. For example, Johnson and colleagues recently reported that OPS and LPS serum and fecal antibody responses in convalescent individuals largely mirror each other but that vibriocidal activity was associated with OPS (35). It would be interesting to evaluate the same samples with respect to motility inhibition.

We also substantiated Bishop and Camilli's claim that antibody-mediated agglutination and motility arrest are in fact separable phenomena (13). Specifically, we demonstrated by video microscopy that exposure of *V. cholerae* to 2D6 Fab fragments resulted in >50% motility inhibition within 5 min and ~75% inhibition by 20 min. We reason that the fact that 2D6 Fab fragments did not arrest bacterial motility to the same degree as 2D6 IgA is indicative of there being at least two mechanisms by which IgA interferes with *V. cholerae* motility. The first is mechanical in nature and involves the "tethering" and cross-linking of *V. cholerae* flagella. SEM analysis of 2D6 IgA-treated cells revealed flagella wrapped around neighboring bacterial bodies and entangled/knotted with other flagella. Flagellar entanglement is not simply an artifact of sample preparation, as we also observed evidence of flagellar tethering via video microscopy. It is not surprising to us that flagellar entanglement would occur in culture, considering that the bacteria swim in excess of 70 μm/s, and their flagella rotate at ~1,700 revolutions/s (33, 40). Moreover, 2D6 has been shown to coat *V. cholerae*'s LPS-sheathed flagellum and would therefore be fully capable of cross-linking the flagellum to other flagella or bacterial bodies (12). What remains unclear is how IgA overcomes the shear force associated with flagellar rotation that would be necessary to promote flagellum-flagellum or flagellum-cell body interactions.

We postulate that the second mechanism of IgA-mediated inhibition of *V. cholerae* motility is due to direct antibody binding to the *V. cholerae* body, which in turn may trigger an outer membrane stress response and/or feedback signaling via the flagellum. While speculative at this stage, the results presented here are reminiscent of studies we have conducted with *S.* Typhimurium in which a monoclonal IgA (Sal4) specific for the O antigen is sufficient to paralyze the bacterium within a matter of minutes (23). Sal4 also affects type 3 secretion system (T3SS) activity, membrane potential, and permeability, as well as exopolysaccharide production (21, 24). Moreover, the association of Sal4 with the *S.* Typhimurium O antigen induces distinct ultrastructural changes in the bacterium's surface morphology, including wrinkles and blebs that are nearly identical to those observed on the surface of *V. cholerae* following 2D6 treatment (20). Membrane bleb formation in particular is indicative of membrane stress (41). Preliminary

transcriptome-based studies are in accordance with the hypothesis that anti-LPS antibodies like 2D6 and ZAC-3 IgA trigger an outer membrane stress response in *V. cholerae* (K. Levinson and N. Mantis, unpublished results).

The studies described in this report were routinely conducted under what are considered non-toxin-inducing conditions (e.g., pH 7.0 and 37°C with aeration) (42, 43). As a result, the bacteria were most certainly devoid of toxin-coregulated pilus (TCP), which is involved in attachment of *V. cholerae* to the intestinal epithelium. TCP also promotes an autoagglutination phenotype that has been proposed to facilitate microcolony formation on mucosal surfaces. It is interesting to speculate how 2D6 IgA might affect TCP-mediated autoagglutination and attachment *in vivo*, considering that TCP forms long filaments that extend well beyond the bacterial surface, compared to 2D6 IgA, which is (theoretically) only 28 nm in length (44) and would simply cap individual LPS molecules (45). The fact that 2D6 IgA protects suckling mice from *V. cholerae* grown under TCP-inducing conditions is evidence that 2D6 trumps TCP, but how exactly that occurs at the cellular and molecular levels remains to be elucidated.

In summary, we propose that protection of the intestinal epithelium from *V. cholerae* infection by S-IgA may be multifactorial, including antibody-induced agglutination, motility arrest, and possibly outer membrane stress. Defining the exact contribution(s) of each of these activities in mucosal immunity will have important implications for vaccine development and assessment. It is clear that vibriocidal activity based on LPS-specific serum IgG and IgM levels in convalescent and vaccinated individuals is a useful but incomplete measure of protection (1, 3, 9). Similarly, determination of total LPS-specific serum IgA and S-IgA titers may reveal only part of the story; we would argue that the "quality" of secretory antibodies might be more important than the actual quantity of antibodies. It is for that reason that it is essential to further identify functional activities associated with protective monoclonal IgA antibodies and then assess these activities on primary polyclonal antibody mixtures. Ultimately, a better understanding of how LPS-specific IgA antibodies interfere with the capacity of *V. cholerae* to colonize the intestinal epithelium will assist in the design of better targeted vaccine strategies and, possibly, the development of surrogate *in vitro* assays that can more effectively predict the protective efficacy of the mucosal antibody responses elicited by candidate cholera vaccines.

REFERENCES

1. **Harris JB, LaRocque RC, Qadri F, Ryan ET, Calderwood SB.** 2012. Cholera. Lancet **379:**2466–2476. http://dx.doi.org/10.1016/S0140-6736(12)60436-X.

2. **Liu L, Johnson HL, Cousens S, Perin J, Scott S, Lawn JE, Rudan I, Campbell H, Cibulskis R, Li M, Mathers C, Black RE, Child Health Epidemiology Reference Group of WHO and UNICEF.** 2012. Global, regional, and national causes of child mortality: an updated systematic analysis for 2010 with time trends since 2000. Lancet **379:**2151–2161. http://dx.doi.org/10.1016/S0140-6736(12)60560-1.

3. **Pasetti MF, Levine MM.** 2012. Insights from natural infection-derived immunity to cholera instruct vaccine efforts. Clin Vaccine Immunol **19:**1707–1711. http://dx.doi.org/10.1128/CVI.00543-12.

4. **Guentzel MN, Berry LJ.** 1975. Motility as a virulence factor for *Vibrio cholerae*. Infect Immun **11:**890–897.

5. **Lee SH, Butler SM, Camilli A.** 2001. Selection for in vivo regulators of bacterial virulence. Proc Natl Acad Sci U S A **98:**6889–6894. http://dx.doi.org/10.1073/pnas.111581598.

6. **Millet YA, Alvarez D, Ringgaard S, von Andrian UH, Davis BM, Waldor MK.** 2014. Insights into *Vibrio cholerae* intestinal colonization from monitoring fluorescently labeled bacteria. PLoS Pathog **10:**e1004405. http://dx.doi.org/10.1371/journal.ppat.1004405.

7. **Ritchie JM, Waldor MK.** 2009. *Vibrio cholerae* interactions with the gastrointestinal tract: lessons from animal studies. Curr Top Microbiol Immunol **337:**37–59. http://dx.doi.org/10.1007/978-3-642-01846-6_2.

8. **Kirn TJ, Bose N, Taylor RK.** 2003. Secretion of a soluble colonization factor by the TCP type 4 pilus biogenesis pathway in *Vibrio cholerae*. Mol Microbiol **49:**81–92. http://dx.doi.org/10.1046/j.1365-2958.2003.03546.x.

9. **Bishop AL, Camilli A.** 2011. *Vibrio cholerae*: lessons for mucosal vaccine design. Expert Rev Vaccines **10:**79–94. http://dx.doi.org/10.1586/erv.10.150.

10. **Centers for Disease Control and Prevention.** 2012. Notes from the field: identification of *Vibrio cholerae* serogroup O1, serotype Inaba, biotype El Tor strain-Haiti, March 2012. MMWR Morb Mortal Wkly Rep **61:**309.

11. **Apter FM, Michetti P, Winner LS, III, Mack JA, Mekalanos JJ, Neutra MR.** 1993. Analysis of the roles of antilipopolysaccharide and anti-cholera toxin immunoglobulin A (IgA) antibodies in protection against *Vibrio cholerae* and cholera toxin by use of monoclonal IgA antibodies in vivo. Infect Immun **61:**5279–5285.

12. **Winner L, III, Mack J, Weltzin R, Mekalanos JJ, Kraehenbuhl JP, Neutra MR.** 1991. New model for analysis of mucosal immunity: intestinal secretion of specific monoclonal immunoglobulin A from hybridoma tumors protects against *Vibrio cholerae* infection. Infect Immun **59:**977–982.

13. **Bishop AL, Schild S, Patimalla B, Klein B, Camilli A.** 2010. Mucosal immunization with *Vibrio cholerae* outer membrane vesicles provides maternal protection mediated by antilipopolysaccharide antibodies that inhibit bacterial motility. Infect Immun **78:**4402–4420. http://dx.doi.org/10.1128/IAI.00398-10.

14. **Leitner DR, Feichter S, Schild-Prufert K, Rechberger GN, Reidl J, Schild S.** 2013. Lipopolysaccharide modifications of a cholera vaccine candidate based on outer membrane vesicles reduce endotoxicity and reveal the major protective antigen. Infect Immun **81:**2379–2393. http://dx.doi.org/10.1128/IAI.01382-12.

15. **Majumdar AS, Dutta P, Dutta D, Ghose AC.** 1981. Antibacterial and antitoxin responses in the serum and milk of cholera patients. Infect Immun **32:**1–8.

16. **Majumdar AS, Ghose AC.** 1981. Evaluation of the biological properties of different classes of human antibodies in relation to cholera. Infect Immun **32:**9–14.

17. **Harris JB, Larocque RC, Chowdhury F, Khan AI, Logvinenko T, Faruque AS, Ryan ET, Qadri F, Calderwood SB.** 2008. Susceptibility to *Vibrio cholerae* infection in a cohort of household contacts of patients with cholera in Bangladesh. PLoS Negl Trop Dis **2:**e221. http://dx.doi.org/10.1371/journal.pntd.0000221.

18. **Patel SM, Rahman MA, Mohasin M, Riyadh MA, Leung DT, Alam MM, Chowdhury F, Khan AI, Weil AA, Aktar A, Nazim M, LaRocque RC, Ryan ET, Calderwood SB, Qadri F, Harris JB.** 2012. Memory B cell responses to *Vibrio cholerae* O1 lipopolysaccharide are associated with protection against infection from household contacts of patients with cholera in Bangladesh. Clin Vaccine Immunol **19:**842–848. http://dx.doi.org/10.1128/CVI.00037-12.

19. **Uddin T, Harris JB, Bhuiyan TR, Shirin T, Uddin MI, Khan AI, Chowdhury F, LaRocque RC, Alam NH, Ryan ET, Calderwood SB, Qadri F.** 2011. Mucosal immunologic responses in cholera patients in Bangladesh. Clin Vaccine Immunol **18:**506–512. http://dx.doi.org/10.1128/CVI.00481-10.

20. **Mantis NJ, Forbes SJ.** 2010. Secretory IgA: arresting microbial pathogens at epithelial borders. Immunol Invest **39:**383–406. http://dx.doi.org/10.3109/08820131003622635.

21. **Amarasinghe JJ, D'Hondt RE, Waters CM, Mantis NJ.** 2013. Exposure of *Salmonella enterica* serovar Typhimurium to a protective monoclonal IgA triggers exopolysaccharide production via a diguanylate cyclase-dependent pathway. Infect Immun **81:**653–664. http://dx.doi.org/10.1128/IAI.00813-12.

22. **Forbes SJ, Bumpus T, McCarthy EA, Corthesy B, Mantis NJ.** 2011. Transient suppression of *Shigella flexneri* type 3 secretion by a protective O-antigen-specific monoclonal IgA. mBio **2(3):**e00042-11. http://dx.doi.org/10.1128/mBio.00042-11.

23. **Forbes SJ, Eschmann M, Mantis NJ.** 2008. Inhibition of *Salmonella enterica* serovar Typhimurium motility and entry into epithelial cells by a protective antilipopolysaccharide monoclonal immunoglobulin A antibody. Infect Immun **76:**4137–4144. http://dx.doi.org/10.1128/IAI.00416-08.

24. **Forbes SJ, Martinelli D, Hsieh C, Ault JG, Marko M, Mannella CA, Mantis NJ.** 2012. Association of a protective monoclonal IgA with the O antigen of *Salmonella enterica* serovar Typhimurium impacts type 3 secretion and outer membrane integrity. Infect Immun **80:**2454–2463. http://dx.doi.org/10.1128/IAI.00018-12.

25. **Wang J, Villeneuve S, Zhang J, Lei P, Miller CE, Lafaye P, Nato F, Szu SC, Karpas A, Bystricky S, Robbins JB, Kovac P, Fournier JM, Glaudemans CP.** 1998. On the antigenic determinants of the lipopolysaccharides of *Vibrio cholerae* O:1, serotypes Ogawa and Inaba. J Biol Chem **273:**2777–2783. http://dx.doi.org/10.1074/jbc.273.5.2777.

26. **Levinson K, Koestler B, Waters C, Mantis N.** 2014. Protective anti-LPS monoclonal antibodies in *Vibrio cholerae*, abstr D-2094. Abstr 114th Gen Meet Am Soc Microbiol. American Society for Microbiology, Washington, DC. http://gm.asm.org.

27. **Mekalanos JJ, Collier RJ, Romig WR.** 1979. Enzymic activity of cholera toxin. II. Relationships to proteolytic processing, disulfide bond reduction, and subunit composition. J Biol Chem **254:**5855–5861.

28. **Miller WG, Lindow SE.** 1997. An improved GFP cloning cassette designed for prokaryotic transcriptional fusions. Gene **191:**149–153. http://dx.doi.org/10.1016/S0378-1119(97)00051-6.

29. **Michetti P, Mahan MJ, Slauch JM, Mekalanos JJ, Neutra MR.** 1992. Monoclonal secretory immunoglobulin A protects mice against oral challenge with the invasive pathogen *Salmonella typhimurium*. Infect Immun **60:**1786–1792.

30. **Mantis NJ, Cheung MC, Neutra MR.** 1999. Selective adhesion of IgA to murine intestinal M cells. Immunol Lett **69:**42.

31. **De Jesus M, Ahlawat S, Mantis NJ.** 17 March 2013. Isolating and immunostaining lymphocytes and dendritic cells from murine Peyer's patches. J Vis Exp http://dx.doi.org/10.3791/50167.

32. **Schindelin J, Arganda-Carreras I, Frise E, Kaynig V, Longair M, Pietzsch T, Preibisch S, Rueden C, Saalfeld S, Schmid B, Tinevez JY, White DJ, Hartenstein V, Eliceiri K, Tomancak P, Cardona A.** 2012. Fiji: an open-source platform for biological-image analysis. Nat Methods **9:**676–682. http://dx.doi.org/10.1038/nmeth.2019.

33. **Shigematsu M, Meno Y, Misumi H, Amako K.** 1995. The measurement of swimming velocity of *Vibrio cholerae* and *Pseudomonas aeruginosa* using the video tracking methods. Microbiol Immunol **39:**741–744. http://dx.doi.org/10.1111/j.1348-0421.1995.tb03260.x.

34. **Liu Z, Miyashiro T, Tsou A, Hsiao A, Goulian M, Zhu J.** 2008. Mucosal penetration primes *Vibrio cholerae* for host colonization by repressing quorum sensing. Proc Natl Acad Sci U S A **105:**9769–9774. http://dx.doi.org/10.1073/pnas.0802241105.

35. **Johnson RA, Uddin T, Aktar A, Mohasin M, Alam MM, Chowdhury F, Harris JB, LaRocque RC, Bufano MK, Yu Y, Wu-Freeman Y, Leung DT, Sarracino D, Krastins B, Charles RC, Xu P, Kovac P, Calderwood SB, Qadri F, Ryan ET.** 2012. Comparison of immune responses to the O-specific polysaccharide and lipopolysaccharide of *Vibrio cholerae* O1 in Bangladeshi adult patients with cholera. Clin Vaccine Immunol **19:**1712–1721. http://dx.doi.org/10.1128/CVI.00321-12.

36. **Mantis NJ, Rol N, Corthesy B.** 2011. Secretory IgA's complex roles in immunity and mucosal homeostasis in the gut. Mucosal Immunol **4:**603–611. http://dx.doi.org/10.1038/mi.2011.41.

37. **Phalipon A, Cardona A, Kraehenbuhl JP, Edelman L, Sansonetti PJ, Corthesy B.** 2002. Secretory component: a new role in secretory IgA-mediated immune exclusion in vivo. Immunity **17:**107–115. http://dx.doi.org/10.1016/S1074-7613(02)00341-2.

38. **Williams RC, Gibbons RJ.** 1972. Inhibition of bacterial adherence by secretory immunoglobulin A: a mechanism of antigen disposal. Science **172:**697–699.

39. **Gustafsson B, Holme T.** 1985. Rapid detection of *Vibrio cholerae* O:1 by motility inhibition and immunofluorescence with monoclonal antibodies. Eur J Clin Microbiol **4:**291–294. http://dx.doi.org/10.1007/BF02013655.

40. **Asai Y, Kojima S, Kato H, Nishioka N, Kawagishi I, Homma M.** 1997. Putative channel components for the fast-rotating sodium-driven flagellar motor of a marine bacterium. J Bacteriol **179:**5104–5110.

41. **Kulp A, Kuehn MJ.** 2010. Biological functions and biogenesis of secreted bacterial outer membrane vesicles. Annu Rev Microbiol **64:**163–184. http://dx.doi.org/10.1146/annurev.micro.091208.073413.

42. **Kirn TJ, Lafferty MJ, Sandoe CM, Taylor RK.** 2000. Delineation of pilin domains required for bacterial association into microcolonies and intestinal colonization by *Vibrio cholerae*. Mol Microbiol **35:**896–910. http://dx.doi.org/10.1046/j.1365-2958.2000.01764.x.

43. **Krebs SJ, Taylor RK.** 2011. Protection and attachment of *Vibrio cholerae* mediated by the toxin-coregulated pilus in the infant mouse model. J Bacteriol **193:**5260–5270. http://dx.doi.org/10.1128/JB.00378-11.

44. **Boehm MK, Woof JM, Kerr MA, Perkins SJ.** 1999. The Fab and Fc fragments of IgA1 exhibit a different arrangement from that in IgG: a study by X-ray and neutron solution scattering and homology modelling. J Mol Biol **286:**1421–1447. http://dx.doi.org/10.1006/jmbi.1998.2556.

45. **Villeneuve S, Souchon H, Riottot MM, Mazie JC, Lei P, Glaudemans CP, Kovac P, Fournier JM, Alzari PM.** 2000. Crystal structure of an anti-carbohydrate antibody directed against *Vibrio cholerae* O1 in complex with antigen: molecular basis for serotype specificity. Proc Natl Acad Sci U S A **97:**8433–8438. http://dx.doi.org/10.1073/pnas.060022997.